RSC Advances

RSC Advances

www.rsc.org/advances

ROYAL SOCIETY OF CHEMISTRY

www.rsc.org/advances

Journal Name

ARTICLE

Synthesis, Crystal Structure and Physical Properties of [Li$_{0.85}$Fe$_{0.15}$OH][FeS]

Xian Zhang,[a] Xiaofang Lai,[a] Na Yi,[b] Jianqiao He,[b] Haijie Chen,[b] Hui Zhang,[b] Jianhua Lin,*[a] Fuqiang Huang*[a,b]

The layered mixed anion compound with the formula [Li$_{0.85}$Fe$_{0.15}$OH][FeS] was synthesized *via* a facile hydrothermal method. [Li$_{0.85}$Fe$_{0.15}$OH][FeS], which is determined by single crystal X-ray diffraction and refined by SHELXTL program, crystallizes in the tetragonal space group of *P4/nmm* (*a* = *b* = 3.6886(3) Å, *c* = 8.915(1) Å, *V* = 121.29(2) Å^3, *Z* = 2). The structure features alternative packed anti-PbO-like [Li$_{0.85}$Fe$_{0.15}$OH] and anti-PbO [FeS] layers. The sample was characterized by Field Emission Scanning Electron Microscopy (FESEM), High-Resolution Transmission Electron Microscopy (HRTEM). Powder X-ray diffraction result confirms the phase purity of the as-synthesized crystals. Temperature-dependent measurements of magnetic susceptibility reveal the presence of paramagnetic-to-ferromagnetic phase transition around 50 K, accompanied by the metal-to-semiconductor phase transition in the temperature-dependent resistance of the [Li$_{0.85}$Fe$_{0.15}$OH][FeS] single crystal.

Introduction

Materials with different structural/functional units can easily integrate the advantages of different structural/functional units, and thus offer multifunctional applications.[1] Layered compounds, with *van der Waals* gaps between layers, have the naturally formed structural/functional units, due to the weak interaction between layers, and hence the weak impact of each packing habits. Among these, the layered compounds with mixed anions can much easier form the structure/functional units, for instance the transparent conductor LaOCuS,[2] the thermoelectric BiOCuSe,[3] the photoelectric Bi$_2$O$_2$S,[4] and the famous superconducting *Ln*OFeAs (*Ln* = La, Ce, Pr, Nd, Sm)[5] and *Ln*OBiS$_2$ (*Ln* = La, Ce, Pr, Nd, Sm),[6] which results in the growing attention that has been received.

Iron-chalcogenide-based materials have received much more attention, due to their rich physical properties. Nowadays, researchers have focused on the new superconductors searching since the discovery of FeSe with a superconducting transition temperature *T$_c$* up to 9 K.[7] External pressure can adjust the superconducting transition temperature from 8 to 37 K,[8] which is attributed to the anion height between Fe and chalcogen layers.[9] In addition to the external pressure, intercalation can also change the anion height by changing the local environment of FeSe slabs, and hence adjust the *T$_c$*.[10] Therefore, intercalation can be understood to be the internal pressure. The tetragonal FeS (mackinawite) is found to be semiconductor.[11] Like the FeSe compound, the physical properties of tetragonal FeS can also be tuned from semiconductor to metallic character by external pressure.[11b] However, few of the intercalation for tetragonal FeS have been reported, which may impact its physical properties.[12]

Recently, the layered [Li$_{1-x}$Fe$_x$OH][Fe$_{1-y}$Li$_y$Se] compound, with mixed anions (OH$^-$ and Se^{2-}) and distinct structural/functional layers, have been successfully synthesized and found to be superconducting under *T$_c$* = 43 K.[12, 13] The compound can be seen as the intercalation of [Li$_{0.8}$Fe$_{0.2}$OH] layers into bulk FeSe. In addition to the superconducting phase transition, the compound also undergoes another magnetic phase transition around 10 K.[13c, 13d] However, the phase transition type remains controversial (ferromagnetism[13d] or anti-ferromagnetism[13c]). Therefore, understanding the physical properties of this type of materials is necessary. The sulfide analog of this type of compound, namely the [Li$_{0.8}$Fe$_{0.2}$OH][FeSe$_{1-x}$S$_x$] powder, also has been reported.[12] However, the crystal structure is mainly determined by powder X-ray diffraction. Overall, exploring new mixed anion compounds containing similar Fe*Q* layers and understanding their physical properties would be instructive.

In this work, we present the single crystal structure and ferromagnetic phase transition of [Li$_{0.85}$Fe$_{0.15}$OH][FeS], which is synthesized *via* the hydrothermal method. The structure features alternative packed [Li$_{0.85}$Fe$_{0.15}$OH] and FeS layers. Both the anti-PbO-like [Li$_{0.85}$Fe$_{0.15}$OH] and anti-PbO FeS layers undergo squashed distortion. The anion height of the FeS layers is 0.138 nm, which is similar to the optimum height for the FeSe-related superconductors. Magnetic measurements indicate the compound is paramagnetic at high temperature, and undergoes a ferromagnetic phase transition around 50 K. Temperature-dependent resistance reveals that the compound has metallic characters at high temperature. A metal-semiconductor transition occurs, accompanying the ferromagnetic transition.

Experimental

Synthesis of [Li$_{0.85}$Fe$_{0.15}$OH][FeS] single crystals. The [Li$_{0.85}$Fe$_{0.15}$OH][FeS] single crystals were synthesized by the

reported method with little modification.[12, 13d] Ten millilitre of deionized water, 0.01 mol of Fe powder and 0.025 mol of thiourea (CH_4N_2S) were added into a 50 mL beaker under stirring. Then, 0.3 mol of $LiOH \cdot H_2O$ powders was added gradually into the beaker. Finally, the reaction mixture was then transferred into a 50-mL Teflon-lined stainless steel autoclave with 75% filling. The reaction was carried out under autogenous pressure at 200 °C for 3 days. After the autoclave was cooled down and depressurized, the lamellar crystals were washed with deionized water for several times and dried with acetone. Then the obtained crystals were kept in the Ar-filled glove box.

Single Crystal X-ray crystallography. Single crystal X-ray diffraction data collection was performed on an *Agilent Super Nova Diffractometer* equipped with graphite-monochromated Mo-$K\alpha$ radiation. The structure of $[Li_{0.85}Fe_{0.15}OH][FeS]$ was solved by direct methods and refined by full-matrix least-squares on F^2 using the SHELXTL program package.[14] Multi-scan absorption corrections were performed. H atoms in the structure are added by calculation. The crystal data and refinement details are presented in Table 1.

Table 1. Crystallographic data and details of the structure refinement for $[Li_{0.85}Fe_{0.15}OH][FeS]$

Compound	$[Li_{0.85}Fe_{0.15}OH][FeS]$
Chemical formula	$[Li_{0.85}Fe_{0.15}OH][FeS]$
Formula weight/g·mol^{-1}	119.19
Crystal system	Tetragonal
a/Å	3.6886(3)
b/Å	3.6886(3)
c/Å	8.915(1)
α/°	90.00
β/°	90.00
γ/°	90.00
Unit cell volume/Å^3	121.29(2)
Temperature/K	180
Space group	*P 4/n m m*
Z	2
Radiation type	Mo Kα
Absorption coefficient	7.530
Calculated density/g·cm^{-3}	3.258
No. of reflections measured	254
No. of independent reflections	121
R_{int}	0.0476
Final R indices [$I>2\sigma(I)$]	0.0303
Final w$R(F^2)$ indices [$I>2\sigma(I)$]	0.0813
Final R indices (all data)	0.0306
Final w$R(F^2)$ indices (all data)	0.0815
Goodness-of-fit on F^2	1.050

Characterization. Inductively Coupled Plasma Mass Spectrometry (ICP-MS) was used to determine the Li/Fe element ratio in the compound. Field Emission Scanning Electron Microscopy (FESEM) images were acquired using FEI Sirion 200 with an energy dispersive X-ray (EDX) analysis. High Resolution Transmission Electron Microscopy (HRTEM) images were taken on JEOL JEM-2100F at an accelerating voltage of 200 kV. HRTEM samples were prepared by dip-casting $[Li_{0.85}Fe_{0.15}OH][FeS]$ crystals (pretreated by grounding) dispersed in ethanol onto carbon-coated copper grids. X-ray diffraction (XRD) patterns were collected on a Bruker D8 Focus X-ray diffractometer equipped with a monochromatized source of Cu Kα radiation (λ= 0.15406 nm) at 1.6 kW (40 kV, 40 mA). The patterns were recorded in a slow-scanning mode with 2θ from 10° to 80° with a scan-rate of 6°/min.

Physical properties measurements. Magnetic properties were studied using a Quantum Design Physical Properties Measurement System (PPMS). Temperature-dependent direct-current (DC) magnetic susceptibility (*M-T*) curve of the sample was measured from 300 to 2 K under 10 Oe magnetic field under zero field cooling (ZFC) and field cooling (FC) conditions. The temperature variation of the resistance, *R(T)*, was measured using the standard two-probe technique by Resistivity model collected on the PPMS. For electric properties measurements, the single crystal was chosen from the as-synthesized crystals. The silver paste was dropped and acting as the contact electrode.

Results and discussion

Hydrothermal method, compared to the traditional high-temperature solid state synthesis, has the advantages in synthesizing meta-stable phases for its mild reaction conditions and kinetics control process. The newly developed hydrothermal synthesis, with the assistance of concentrated base (LiOH) as the mineralizer, can efficiently produce the superconducting $[Li_{0.8}Fe_{0.2}OH][FeSe]$,[13a, 13c] photoelectric Bi_2O_2S.[4b] With CH_4N_2S as a sulfur source, which gradually releases S at a relatively higher temperature of 200 °C than the melting point of 182 °C, we synthesized the $[Li_{0.85}Fe_{0.15}OH][FeS]$ single crystals. As shown in **Figure 1a**, the SEM image indicates the crystal features well-defined square plates. EDX analysis (**Figure 1b**) of a number of crystals reveals the presence of the Fe, S and O elements, and the relative ratio is about 1.18/1/1.05. The elemental mapping of the single crystal of the title compound declares the uniform composition of the crystal, as shown in **Figure 1c**. The ICP-MS results indicate the Li/Fe element ratio is 1/1.4. The phase purity of the as-synthesized crystals was checked by powder X-ray diffraction, as shown in the **Figure 1d**. All the peaks can be indexed by the *P4/nmm* space group with the lattice parameters of $a = b = 3.7$ Å, $c = 8.9$ Å, and $V = 121.8$ Å^3, indicating its phase purity. Besides, the as-synthesized $[Li_{0.85}Fe_{0.15}OH][FeS]$ may be isostructural with the reported superconducting $[Li_{0.8}Fe_{0.2}OH][FeSe]$ (*P4/nmm*, $a = b = 3.8038$ Å. $c = 9.2210$ Å).[13c, 13d] The sharp peaks show the high degree of crystallinity of the $[Li_{0.85}Fe_{0.15}OH][FeS]$ crystals. The HRTEM image shows a set of high resolution lattice planes with the inter-planar distance of 0.297 nm (**Figure 2a**), corresponding to the (003) plane of the model obtained by powder XRD. The independent well-defined diffraction points in the SAED image have four-fold axis, consisting with the space group of *P 4/nmm*. The inter-point distance is measured, and the point can be indexed by the *P4/nmm* space group, as show in **Figure 2b.**
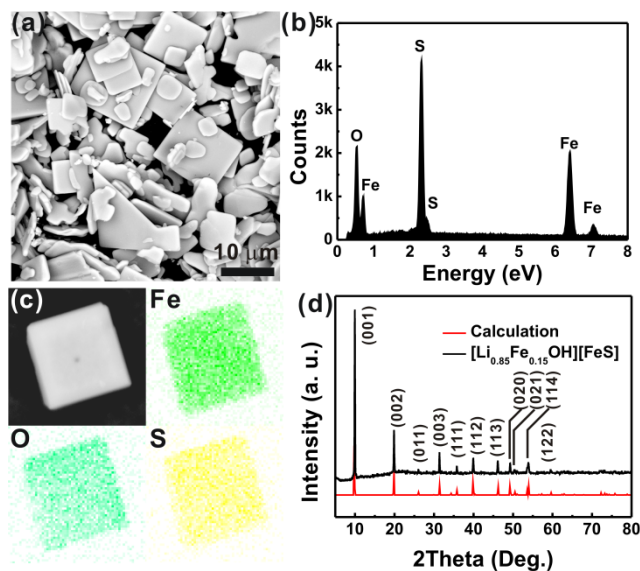
Figure 1. (a) FESEM of $[Li_{0.85}Fe_{0.15}OH][FeS]$ single crystals. (b) EDX results of the single crystals. (c) Elemental distribution of the Fe, O and S elements in the $[Li_{0.85}Fe_{0.15}OH][FeS]$ single crystal. (d) X-ray diffraction of $[Li_{0.85}Fe_{0.15}OH][FeS]$
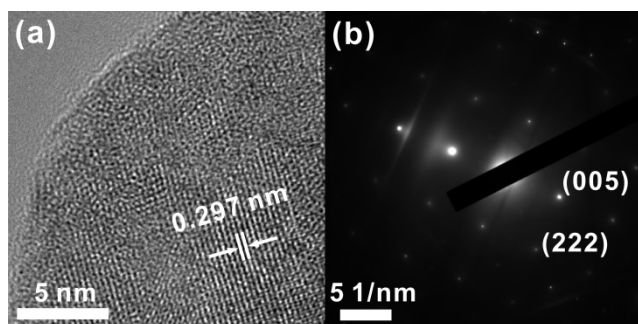

Figure 2. (a) HRTEM image and SAED (b) of $[Li_{0.85}Fe_{0.15}OH][FeS]$ compound.

The structure of the compound is shown in **Figure 3**. The compound, which is isostructural to the superconducting $[Li_{0.8}Fe_{0.2}OH][FeSe]$ compound, crystallizes in the tetragonal space group *P4/nmm* with the lattice constant of $a = b = 3.6886(3)$ Å, $c = 8.915(1)$ Å. The structure features alternative stacked $[Li_{0.85}Fe_{0.15}OH]$ and $[FeS]$ layers, as shown in **Figure 3a**. The $[FeS]$ layer has the anti-PbO-type structure, while the $[Li_{0.85}Fe_{0.15}OH]$ layer has the anti-PbO-like structure, as shown in **Figure 3b & 3c**. There are one unique Li *Wyckoff* site (2*a*), two unique Fe *Wyckoff* sites (Fe1 at 2*b*, Fe2 at 2*a*), one unique H *Wyckoff* sites (2*c*), one unique O *Wyckoff* sites (2*c*) and one unique S *Wyckoff* sites (2*c*). The Fe1 atom is coordinated to four S atoms to form the distorted tetrahedron (**Figure 4a**). The Fe-S distance is 2.2486(7) Å, which is comparable to the Fe-S distance in FeS (2.231 Å).[15] The largest angle in the distorted $[FeS_4]$ tetrahedron is 110.2°, meaning the $[FeS_4]$ tetrahedron is squashed along *c* axis. Those squashed $[FeS_4]$ tetrahedra connect with each other *via* edge sharing to build up the $[FeS]$ layers. The anion height of the squashed FeS layers is 0.138 nm, which is the optimum value for the superconducting FeSe.[9] This kind of $[FeS]$ layer also shows up in the tetragonal FeS.[15a]

Note that the $[FeS_4]$ tetrahedra in the binary FeS compound also undergo the squashed distortion along *c* axis with the largest S-Fe-S angle of 111.1°. The Li atom, partially replaced by Fe2 atom, coordinates to four O atoms to form the highly distorted tetrahedron (**Figure 4b**). The Li/Fe-O distance is 1.977(2) Å, which is comparable to the Li-O distance in Li_2O (1.996 Å)[16] but shorter than the Fe-O distance in FeO (2.171 Å).[17] The largest O-Li/Fe-O angle in the $[Li/FeO_4]$ tetrahedra is 137.8°, indicating the higher degree of squashed distortion of $[Li/FeO_4]$ tetrahedra than $[FeS_4]$ tetrahedra.

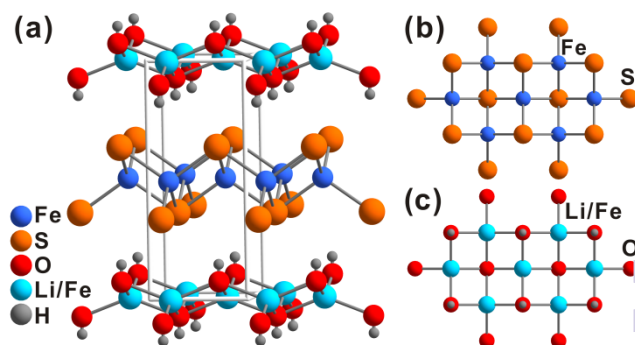**Figure 3**. (a) Schematical diagram of the crystal structure of $[Li_{0.85}Fe_{0.15}OH][FeS]$. (b) The $[FeS]$ layer viewed along *c* axis. (c) The $[Li_{0.85}Fe_{0.15}OH]$ layer viewed along *c* axis.
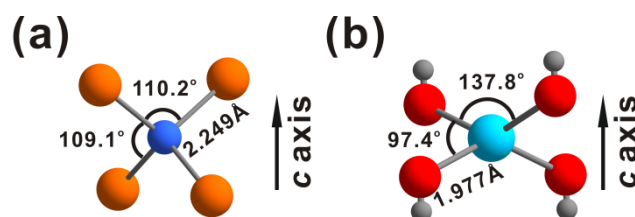

Figure 4. (a) The distorted $[FeS_4]$ tetrahedra. (b) The distorted $[Li_{0.85}Fe_{0.15}(OH)_4]$ tetrahedra.

The magnetic properties of the $[Li_{0.85}Fe_{0.15}OH][FeS]$ compound are measured, and the temperature-dependent zero-field-cooling (ZFC) and field-cooling (FC) magnetization at a magnetic field of 10 Oe for the compound are plotted in **Figure 5a**. Clearly, no typical magnetic phase-transition occurs in the temperature range from 300 K to 50 K. This indicates the dominance of paramagnetic contribution at high temperature. After the temperature cooled down to 50 K, the magnetization increases sharply with the decrease of temperature. This implies the magnetic phase transition, from the paramagnetic to ferromagnetic phase, occurs in the low temperature region. The inverse magnetic susceptibility *vs* temperature plot (**Figure 5b**) shows linear dependence in the temperature range from 300 K to 50 K, indicating that the $[Li_{0.85}Fe_{0.15}OH][FeS]$ is a paramagnetic compound. The field-dependence of the magnetization of the compound at 300 K and 2 K are described in **Figure 5c**. The linear relationship of *H vs M* at 300 K also confirms the paramagnetic characters at high temperature. The obedience of linear relationship of *M vs H* at 2 K, with slightly bending, further confirms the occurrence of magnetic phase transition at low temperature. The zoomed *M vs H* curves at 300 K and 2 K are described in **Figure 5d**. Clear magnetic hysteresis shows up at 2 K, which is different from the *M vs H* curve at 300 K (linear). The coercive field is about 25 Oe, and the remanence is about 8 memu/g. Overall, the

[Li$_{0.85}$Fe$_{0.15}$OH][FeS] compound shows paramagnetic characters at high temperature and ferromagnetic characters at low temperature with the T_{fm} about 50 K. This ferromagnetic transition is also reported in the [Li$_{0.8}$Fe$_{0.2}$OH][FeSe] compound, which has a lower transition temperature (~ 10 K).[13d] The absence of superconductivity of the title compound can attributed to local structure distortion effect or chemical pressure effect which arises by substituting the smaller S atoms for the Se atoms.[12, 18, 19]
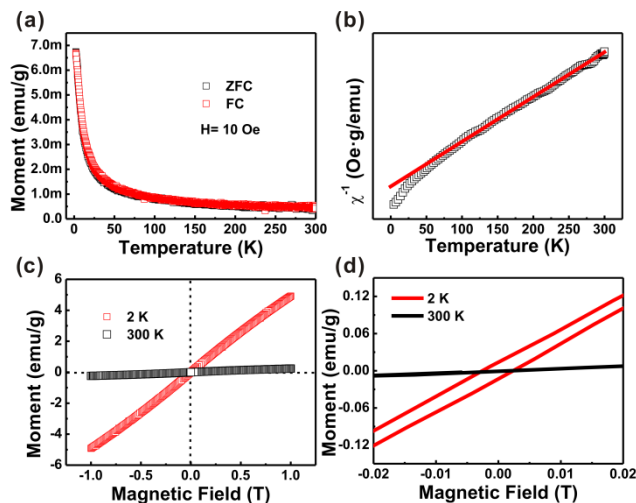
Figure 5. (a) Temperature-dependence of the magnetization of the [Li$_{0.85}$Fe$_{0.15}$OH][FeS] compound. (b) The inverse magnetic susceptibility *vs* temperature plot. The red line is the linear fit of the magnetic susceptibility data from 300 K to 50 K. (c) Magnetic hysteresis of the [Li$_{0.85}$Fe$_{0.15}$OH][FeS] compound under 2 K and 300 K. (d) The zoomed magnetic hysteresis of the [Li$_{0.85}$Fe$_{0.15}$OH][FeS] compound under 2 K and 300 K.

Temperature-dependent resistance of the [Li$_{0.85}$Fe$_{0.15}$OH][FeS] single crystal is shown in **Figure 6.** The resistance decreases with the decrease of the temperature in the range of 250 K to 50 K, indicating the metallic property of the compound in this temperature range. However, the resistance increases upon further cooling of the crystal, meaning the semiconducting-like phase transition occurs. There are two well-known models that can be used to describe the semiconducting transport. The first one is the small polaron hopping (SPH) model, in which the $\rho(T)$ is expressed as $\rho(T)/T \propto exp(E_P/k_BT))$ with the E_p being the activation energy.[20] The other one is the variable range hopping (VRH) model, in which the $\rho(T)$ is expressed as $\rho(T) \propto exp(T_0/T)^{1/4}$ with the T_0 being the characteristic temperature.[21] The resistance data in the temperature range from 50 K to 4 K are fitted in both SPH and VRH models, as shown in **Figure 6b and 6c**, respectively. Apparently, the resistivity can be fitted by using the VRH model but not the SPH model. This indicates the compound possesses a metal-to-semiconductor phase transition at low temperature (~ 50 K). The metal-to-semiconductor temperature consists with the magnetic phase transition temperature. Therefore, we propose that the increase of the resistance of the compound is caused due to the magnetic phase transition in the compound.
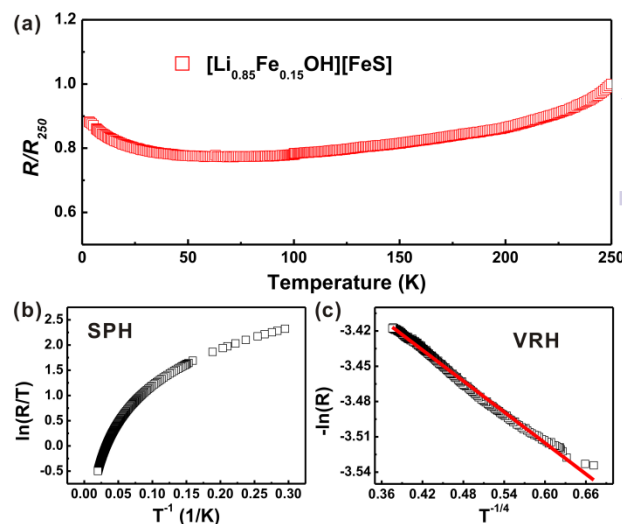

Figure 6. (a) Temperature-dependence of resistance of the [Li$_{0.85}$Fe$_{0.15}$OH][FeS] single crystal. (b) $ln(R/T)$ *vs* T^{-1} plot of the SPH model. (c) $-ln(R)$ *vs* $T^{-1/4}$ plot of the VRH model.

Conclusions

In summary, we have successfully synthesized the layered mixed anion compound with the formula [Li$_{0.85}$Fe$_{0.15}$OH][FeS] *via* hydrothermal method. The compound crystallized in the tetragonal space group of *P4/nmm* ($a = b = 3.6886$ (3) Å, $c = 8.915$ (1) Å). The structure features the alternative packed anti-PbO-like [Li$_{0.85}$Fe$_{0.15}$OH] and anti-PbO [FeS] layers. The phase purity of the as-synthesized crystals is confirmed by PXRD. The compound shows paramagnetic properties at high temperature and a ferromagnetic phase transition around 50 K. Accordingly, the metal-to-semiconductor phase transition was found at this temperature in the temperature-dependent resistance of the [Li$_{0.85}$Fe$_{0.15}$OH][FeS] single crystal.

Acknowledgements

Notes and references

a Beijing National Laboratory for Molecular Sciences and State Key Laboratory of Rare Earth Materials Chemistry and Applications, College of Chemistry and Molecular Engineering, Peking University, Beijing 100871, China.
b CAS Key Laboratory of Materials for Energy Conversion and State Key Laboratory of High Performance Ceramics and Superfine Microstructure, Shanghai Institute of Ceramics, Chinese Academy of Sciences, Shanghai 200050, P. R. China.

1. (a) X. Zhang, J. Q. He, W. Chen, K. T. Zhang, C. Zheng, J. L. Sun, F. H. Liao, J. H. Lin and F. Q. Huang, *Chem. Eur. J.*, 2014, 20, 5977-5982. (b) X. Zhang, W. Chen, D. J. Mei, C. Zheng, F. H. Liao,

Y. T. Li, J. H. Lin and F. Q. Huang, *J. Alloys Compd*, 2014, **610**, 671-675. (c) M. L. Liu, I. W. Chen, F. Q. Huang and L. D. Chen, *Adv. Mater.*, 2009, **21**, 3808-3812.

2. (a) C. Doussier-Brochard, B. Chavillon, L. Cario and S. Jobic, *Inorg. Chem.*, 2010, **49**, 3074-3076. (b) K. Takase, K. Sato, O. Shoji, Y. Takahashi, Y. Takano, K. Sekizawa, Y. Kuroiwa and M. Goto, *Appl. Phys. Lett.*, 2007, **90**, 3. (c) Y. Goto, M. Tanaki, Y. Okusa, T. Shibuya, K. Yasuoka, M. Matoba and Y. Kamihara, *Appl. Phys. Lett.*, 2014, **105**, 4. (d) H. Hiramatsu, H. Yanagi, T. Kamiya, K. Ueda, M. Hirano and H. Hosono, *Chem. Mater.*, 2008, **20**, 326-334. (e) S. Inoue, K. Ueda, H. Hosono and N. Hamada, *Phys. Rev. B*, 2001, **64**, 5.

3. (a) J. Li, J. H. Sui, Y. L. Pei, C. Barreteau, D. Berardan, N. Dragoe, W. Cai, J. Q. He and L. D. Zhao, *Energy Environ. Sci.*, 2012, **5**, 8543-8547. (b) F. Li, J. F. Li, L. D. Zhao, K. Xiang, Y. Liu, B. P. Zhang, Y. H. Lin, C. W. Nan and H. M. Zhu, *Energy Environ. Sci.*, 2012, **5**, 7188-7195. (c) L. D. Zhao, J. Q. He, D. Berardan, Y. H. Lin, J. F. Li, C. W. Nan and N. Dragoe, *Energy Environ. Sci.*, 2014, **7**, 2900-2924.

4. (a) A. L. Pacquette, H. Hagiwara, T. Ishihara and A. A. Gewirth, *J. Photochem. Photobiol., A*, 2014, **277**, 27-36. (b) X. Zhang, Y. Liu, G. Zhang, Y. Wang, H. Zhang and F. Huang, *ACS Appl. Mater. Interfaces*, 2015, **7**, 4442-4448.

5. Y. Kamihara, T. Watanabe, M. Hirano and H. Hosono, *J. Am. Chem. Soc.*, 2008, **130**, 3296-3297. (b) G. F. Chen, Z. Li, D. Wu, G. Li, W. Z. Hu, J. Dong, P. Zheng, J. L. Luo and N. L. Wang, *Phys. Rev. Lett.*, 2008, **100**, 4. (c) Z. A. Ren, J. Yang, W. Lu, W. Yi, G. C. Che, X. L. Dong, L. L. Sun and Z. X. Zhao, *Mater. Res. Innovations*, 2008, **12**, 105-106. (d) Z. A. Ren, J. Yang, W. Lu, W. Yi, X. L. Shen, Z. C. Li, G. C. Che, X. L. Dong, L. L. Sun, F. Zhou and Z. X. Zhao, *Europhys. Lett.*, 2008, **82**, 2. (e) X. H. Chen, T. Wu, G. Wu, R. H. Liu, H. Chen and D. F. Fang, *Nature*, 2008, **453**, 761-762.

6. (a) R. Jha, A. Kumar, S. K. Singh and V. P. S. Awana, *J. Supercond. Novel Magn.*, 2013, **26**, 499-502. (b) B. Li, Z. W. Xing and G. Q. Huang, *Europhys. Lett.*, 2013, **101**, 5. (c) G. K. Selvan, M. Kanagaraj, S. E. Muthu, R. Jha, V. P. S. Awana and S. Arumugam, *Phys. Status Solidi RRL*, 2013, **7**, 510-513. (d) J. Xing, S. Li, X. X. Ding, H. Yang and H. H. Wen, *Phys. Rev. B*, 2012, **86**, 5. (e) X. Lin, X. X. Ni, B. Chen, X. F. Xu, X. X. Yang, J. H. Dai, Y. K. Li, X. J. Yang, Y. K. Luo, Q. Tao, G. H. Cao and Z. A. Xu, *Phys. Rev. B*, 2013, **87**, 4.

7. F. C. Hsu, J. Y. Luo, K. W. Yeh, T. K. Chen, T. W. Huang, P. M. Wu, Y. C. Lee, Y. L. Huang, Y. Y. Chu, D. C. Yan and M. K. Wu, *Proc. Natl. Acad. Sci. U. S. A*, 2008, **105**, 14262-14264.

8. (a) Y. Mizuguchi, F. Tomioka, S. Tsuda, T. Yamaguchi and Y. Takano, *Appl. Phys. Lett.*, 2008, **93**, 3. (b) S. Medvedev, T. M. McQueen, I. A. Troyan, T. Palasyuk, M. I. Eremets, R. J. Cava, S. Naghavi, F. Casper, V. Ksenofontov, G. Wortmann and C. Felser, *Nat. Mater.*, 2009, **8**, 630-633.

9. Y. Mizuguchi, Y. Hara, K. Deguchi, S. Tsuda, T. Yamaguchi, K. Takeda, H. Kotegawa, H. Tou and Y. Takano, *Supercond. Sci. Technol.*, 2010, **23**, 5.

10. (a) M. H. Fang, H. D. Wang, C. H. Dong, Z. J. Li, C. M. Feng, J. Chen and H. Q. Yuan, *Europhys. Lett.*, 2011, **94**, 6. (b) A. Krzton-Maziopa, Z. Shermadini, E. Pomjakushina, V. Pomjakushin, M.

Bendele, A. Amato, R. Khasanov, H. Luetkens and K. Conder, *J. Phys.: Condens. Matter*, 2011, **23**, 4. (c) A. F. Wang, J. J. Ying, Y. J. Yan, R. H. Liu, X. G. Luo, Z. Y. Li, X. F. Wang, M. Zhang, G. J. Ye, P. Cheng, Z. J. Xiang and X. H. Chen, *Phys. Rev. B*, 2011, **83**, 4. (d) J. G. Guo, S. F. Jin, G. Wang, S. C. Wang, K. X. Zhu, T. T. Zhou, M. He and X. L. Chen, *Phys. Rev. B*, 2010, **82**, 4.

11. (a) S. J. Denholme, S. Demura, H. Okazaki, H. Hara, K. Deguchi, M. Fujioka, T. Ozaki, T. Yamaguchi, H. Takeya and Y. Takano, *Mater. Chem. Phys.*, 2014, **147**, 50-56. (b) S. J. Denholme, H. Okazaki, S. Demura, K. Deguchi, M. Fujioka, T. Yamaguchi, H. Takeya, M. ElMassalami, H. Fujiwara, T. Wakita, T. Yokoya and Y. Takano, *Sci. Technol. Adv. Mater.*, 2014, **15**, 055007.

12. X. F. Lu, N. Z. Wang, X. G. Luo, G. H. Zhang, X. L. Gong, F. Q. Huang and X. H. Chen, *Phys. Rev. B*, 2014, **90**, 214520.

13. (a) X. F. Lu, N. Z. Wang, G. H. Zhang, X. G. Luo, Z. M. Ma, B. Lei, F. Q. Huang and X. H. Chen, *Phys. Rev. B*, 2014, **89**, 5. (b) C. Heil, L. Boeri, H. Sormann, W. von der Linden and M. Aichhorn, *Physical Review B*, 2014, **90**, 8. (c) X. F. Lu, N. Z. Wang, H. W. Y. P. Wu, D. Zhao, X. Z. Zeng, X. G. Luo, T. Wu, W. Bao, G. H. Zhang, F. Q. Huang, Q. Z. Huang and X. H. Chen, *Nat Mater*, 2015, **14**, 325-329. (d) U. Pachmayr, F. Nitsche, H. Luetkens, S. Kamusella, F. Brückner, R. Sarkar, H.-H. Klauss and D. Johrendt, *Angew. Chem. Inter. Ed.*, 2015, **54**, 293-297.

14. G. Sheldrick, SHELXTL NT Version 5.1. Program for Solution and Refinement of Crystal Structures. *University of Göttingen, Germany* 1997.

15. (a) R. A. Berner, *Science*, 1962, **137**, 669. (b) A. R. Lennie, S. A. T. Redfern, P. F. Schofield and D. J. Vaughan, *Mineral. Mag.*, 1995, **59**, 677-683. (c) I. T. Sines, D. D. Vaughn Ii, R. Misra, E. J. Popczun and R. E. Schaak, *J. Solid State Chem.*, 2012, **196**, 17-20.

16. W. I. F. David, M. O. Jones, D. H. Gregory, C. M. Jewell, S. R. Johnson, A. Walton and P. P. Edwards, *J. Am. Chem. Soc.*, 2007, **129**, 1594-1601.

17. H. Fjellvag, F. Gronvold, S. Stolen and B. Hauback, *J. Solid State Chem.*, 1996, **124**, 52-57.

18. Y. Mizuguchi, F. Tomioka, S. Tsuda, T. Yamaguchi, Y. Takano, *J. Phys. Soc. Jpn.*, 2009, **78**, 074712.

19. H. Lei, M. Abeykoon, E. S. Bozin, K. Wang, J. B. Warren, C. Petrovic, *Phys. Rev. Lett.,* 2011, **107**, 137002

20. N. Mott, E. Davis, Electrical processes in non-crystalline materials. *Clarendon, Oxford* 1971, **152**.

21. N. Mott, *J. Non-Cryst. Solids,* 1968, **1**, 1-17.